

Numerical Evaluation of One-Loop Diagrams Near Exceptional Momentum Configurations *

W. Giele^a, E.W.N. Glover^b and G. Zanderighi^a

^aFermilab, Batavia IL 60150, USA

^bDepartment of Physics, University of Durham, Durham DH1 3LE, England

One problem which plagues the numerical evaluation of one-loop Feynman diagrams using recursive integration by part relations is a numerical instability near exceptional momentum configurations. In this contribution we will discuss a generic solution to this problem. As an example we consider the case of forward light-by-light scattering.

1. Introduction

By using recursion relations based on the integration by part techniques [1] a general algorithm can be constructed to numerically evaluate the finite part of one loop tensor N -point integrals [2]. The numerical implementation is straightforward. However, for specific configurations of the external momenta, the recursion relations build up a numerical instability. Phenomenologically, these exceptional kinematics are characterized by such configurations as mass thresholds, forward scattering and planar event where a parameter tends to zero (for example the scattering angle). In this contribution, we will discuss how to modify the recursion relations to produce expansion formulae in the small parameter. This is an extension of the techniques developed in ref. [3] (see also ref. [4]) and allows the evaluation of tensor loop integrals at/near exceptional momenta configurations. As an example, we work out in some detail forward light by light scattering through a massless fermion loop: $\gamma\gamma \rightarrow \gamma\gamma$. The generalization to massive particles with mass thresholds and processes with larger multiplicities is in principle straightforward.

2. Exceptional Recursion Relations

The dimensionality of space-time fixes the number of momentum vectors needed to form a

*Talk given at the 7th DESY Workshop on Elementary Particle Theory, Loops and Legs in Quantum Field Theory, Zinnowitz 2004.

basis set in Minkowski space. As a consequence the integration by part recursion relations fall into three categories depending on the number of external legs, N , in the loop graph. These categories are: $N \leq 5$, $N = 6$ and $N \geq 7$.

At the center of the recursion relations is the so-called kinematic matrix

$$S_{ij} = (q_i - q_j)^2 - m_i^2 - m_j^2, \quad (1)$$

where q_i is the momentum flow through and m_i the mass of propagator i . For the three aforementioned categories of recursion relations, the kinematic matrix has the following properties:

$N \leq 5$: Both the inverse of the kinematic matrix and the Gram determinant exist for non-exceptional momentum configurations. The Gram determinant is proportional to

$$B = \sum_i b_i = \sum_{ij} S_{ij}^{-1}. \quad (2)$$

For momentum configurations close to exceptional kinematics the B parameter tends to zero. Both the recursion relations and the basis set of loop integrals become numerically unstable in this limit. We need to setup a recursion relation which generates an expansion in B .

$N = 6$: In this case, the inverse of the kinematic matrix still exists for non-exceptional momentum configurations. However, $B =$

$\sum S_{ij}^{-1} = 0$ for all momentum configurations. This leads to a different set of recursion relations. Momentum configurations close to exceptional kinematics are now characterized by small eigenvalues of the kinematic matrix. In other words, the numerical determination of its inverse becomes unstable. We need to setup a recursion relation which generates an expansion in the small eigenvalue(s) of the kinematic matrix.

$N \geq 7$: Here the kinematic matrix is singular for all momentum configurations. Note that we do not need any special recursion relations since the standard recursion relations are numerically stable.

As we look at changing kinematic behaviour as the multiplicity increases, we also see how to construct the recursion relations near exceptional kinematics. Specifically, when we are exactly at an exceptional momentum configuration for $N \leq 5$, i.e. $B = 0$, we can use the $N = 6$ recursion relations which were constructed on the premise that $B = 0$. Similarly, for $N = 6$, at the exceptional momentum configurations the $N \geq 7$ recursion relations can be used.

However, we are interested in the phase space regions *close* to the exceptional momentum configurations. It is clear how to construct the appropriate recursion relations in these regions. We need to rewrite the $N \leq 5$ recursion relation as the $N = 6$ recursion relation plus terms proportional to B (i.e. the Gram determinant). As we will see in the next section, this leads to an expansion formula in B , enabling us to evaluate the loop graph near the exceptional configurations with arbitrary precision. Equivalently, we can rewrite the $N = 6$ recursion relation into the $N \geq 7$ recursion relations plus terms proportional to the small eigenvalue(s). This leads to an expansion in the small eigenvalue(s).

3. Forward $\gamma\gamma \rightarrow \gamma\gamma$ Scattering

In this section we work out the simple example of light-by-light scattering through a massless fermion loop. The analytic answers for the

helicity amplitudes are well known. Some helicity amplitudes, such as $\gamma^+\gamma^+ \rightarrow \gamma^-\gamma^-$ are constants, independent of the underlying kinematics. Other helicity configurations give simple behaviour which is logarithmically divergent as the scattering angle goes to zero. Applying the recursion algorithm of Ref. [2] to this process leads to a numerical evaluation of the amplitudes. However, when the scattering angle becomes small the algorithm becomes numerically unstable (see Figs. 4 and 5). The reason is twofold. First of all some of the recursion relations depend on the inverse of the B parameter

$$B = \frac{2}{s} + \frac{2}{t} = -\frac{2u}{st} = -\frac{2}{s} \left(\frac{1 - \cos\theta}{1 + \cos\theta} \right) \quad (3)$$

which for small scattering angle θ tends to zero. Secondly, one of the basis integrals, i.e. the endpoint of the recursion relation, becomes unstable. More precisely, the six-dimensional box integral has a numerically unstable form (see Figs. 2 and 3):

$$\begin{aligned} & \lim_{sB \rightarrow 0} I(6; 1, 1, 1, 1) \\ &= \lim_{sB \rightarrow 0} \frac{-1}{tsB} \left[\log^2 \left(1 - \frac{sB}{2} \right) - 2\pi i \log \left(1 - \frac{sB}{2} \right) \right] \\ &= \frac{i\pi}{s}. \end{aligned} \quad (4)$$

As discussed in Sec. 2, the solution is to derive an exceptional recursion relation: the B -expansion relations. This is quite straightforward. We use the $N = 6$ recursion relation plus a correction term proportional to B :

$$\begin{aligned} I(D; \nu_1, \nu_2, \nu_3, \nu_4) = & \\ & b_1 I(D; \nu_1 - 1, \nu_2, \nu_3, \nu_4) \\ & + b_2 I(D; \nu_1, \nu_2 - 1, \nu_3, \nu_4) \\ & + b_3 I(D; \nu_1, \nu_2, \nu_3 - 1, \nu_4) \\ & + b_4 I(D; \nu_1, \nu_2, \nu_3, \nu_4 - 1) \\ & + B(D + 1 - \sigma) I(D + 2; \nu_1, \nu_2, \nu_3, \nu_4) \end{aligned} \quad (5)$$

where

$$I(D; \nu_1, \nu_2, \nu_3, \nu_4) = \int \frac{d^D l}{i\pi^{D/2}} \frac{1}{d_1^{\nu_1} d_2^{\nu_2} d_3^{\nu_3} d_4^{\nu_4}}, \quad (6)$$

$\sigma = \sum \nu_i$ and $d_i = (l + q_i)^2 - m_i^2$ the appropriate propagator. This integral depends on the two Mandelstam invariants, s and t .

This relation is exact for $N \leq 6$ in any momentum configuration. However, unlike the usual recursion relations it has no termination point. For example

$$\begin{aligned} I(6; 1, 1, 1, 1) = & \\ & b_1 I(6 - 2\epsilon; 0, 1, 1, 1) + b_2 I(6 - 2\epsilon; 1, 0, 1, 1) \\ & + b_3 I(6 - 2\epsilon; 1, 1, 0, 1) + b_4 I(6 - 2\epsilon; 1, 1, 1, 0) \\ & + (3 - 2\epsilon)BI(8 - 2\epsilon; 1, 1, 1, 1). \end{aligned} \quad (7)$$

The box integral $I(8 - 2\epsilon; 1, 1, 1, 1)$ can be expressed in terms of 8-dimensional triangles (proportional to B) and a 10-dimensional box integral (proportional to B^2). By iterating this process, the scalar box is expressed as a series of triangles with increasing factors of B . In the case of the massless 6-dimensional box we simply get:

$$\begin{aligned} I(6; 1, 1, 1, 1) & \\ = \frac{2}{s} & \left[\sum_{m=0}^M B^m a_m I(6 + 2m - 2\epsilon; 0, 1, 1, 1) \right] \\ + \frac{2}{t} & \left[\sum_{m=0}^M B^m a_m I(6 + 2m - 2\epsilon; 1, 0, 1, 1) \right] \\ + \mathcal{O}(B^{M+1}) & \end{aligned} \quad (8)$$

with a_m the expansion coefficients generated from the last term in eq. 7. In other words we can evaluate the 6-dimensional box integral in the forward scattering region as an series expansion in B , with each coefficient given as triangle integrals with one offshell leg. If the scattering angle is small, not many iterations are needed for an accurate evaluation of the box diagram. This is illustrated in Fig. 1. Of course, for large B , the unmodified integration by parts relations are completely stable.

Note that the triangles appearing in the B -expansion relations are all UV divergent. However, order by order in B these divergences cancel in the sums (because by construction the original integrals are UV finite.) This means we can use a regulated expressions for a_m and the triangles integrals. A complication is that the factor a_m itself is dependent on the dimension. This means that the limit $\epsilon \rightarrow 0$ has to be taken after the UV divergences have been cancelled by adding different triangles. An important property of the coef-

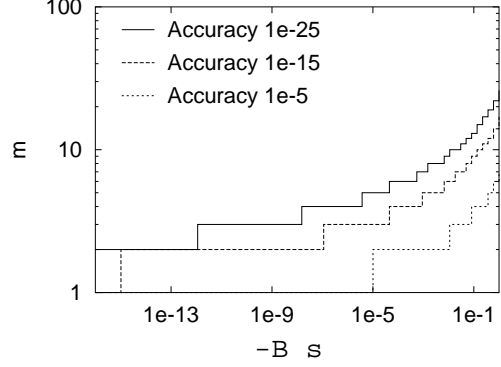


Figure 1. The value of $-sB$ vs the depth of expansion m needed to evaluate the scalar box integral $I(6; 1, 1, 1, 1)$ with a relative accuracy of 10^{-25} , 10^{-15} and 10^{-5} .

ficient a_m is that it is a function of the expansion depth m and the value of $D - \sigma$ where both D and σ are given by the triangle the coefficient is multiplying. The regulated expression to be used in the B -expansion relations is given by

$$\begin{aligned} J_m(D; \nu_1, \nu_2, \nu_3) \equiv a_m I(D + 2m; \nu_1, \nu_2, \nu_3) = & \\ 2^m \frac{(-1)^\sigma Q^{2m}}{\Gamma(\sigma + 2n)} (\nu_2)_n (\nu_3)_n (\sigma/2 + n - m)_m & \\ \times (2\Psi(\sigma + 2n) + \Psi(n + 1) + \Psi(\sigma/2 + n - m) & \\ - \Psi(\nu_2 + n) - \Psi(\nu_3 + n) - \Psi(\sigma/2 + n) & \\ - \log(-Q^2) + \gamma_E) & \end{aligned} \quad (9)$$

where n is given by the relation $D = 2(\sigma + n)$, the Pochhammer's symbol $(n)_m = \Gamma(n + m)/\Gamma(n)$, the Euler constant γ_E and the Digamma function $\Psi(x) = d \log(\Gamma(x))/dx$. As indicated in the notation, in the algorithmic expansion we only need to keep track of the tuple $(m, D, \nu_1, \nu_2, \nu_3)$ in order to evaluate $J_m(D; \nu_1, \nu_2, \nu_3)$. For example, the B -expansion of $I(8; 2, 1, 1, 1)$ using Eq. (5) now becomes

$$\begin{aligned} I(8, 2, 1, 1, 1) = b_1 \sum_{m=0}^M B^m J_m(8; 0, 1, 1, 1) & \\ + b_2 \sum_{m=0}^M B^m [J_m(8; 2, 0, 1, 1) + b_1 J_m(8; 1, 0, 1, 1)] & \end{aligned}$$

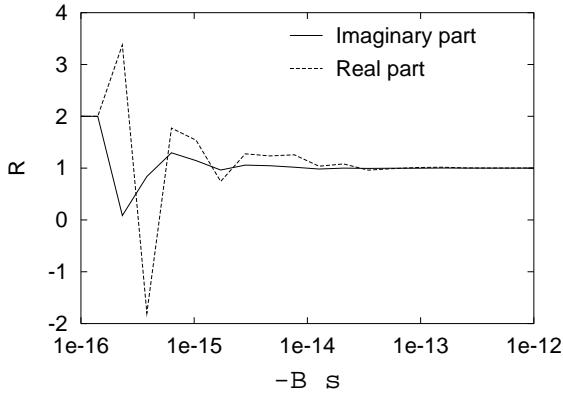


Figure 2. The value of $-sB$ vs the ratio of the standard recursion result and the B -expansion result for $I(6; 1, 1, 1, 1)$.

$$\begin{aligned}
 & + b_3 \sum_{m=0}^M B^m [J_m(8; 2, 1, 0, 1) + b_1 J_m(8; 1, 1, 0, 1)] \\
 & + b_4 \sum_{m=0}^M B^m [J_m(8; 2, 1, 1, 0) + b_1 J_m(8; 1, 1, 1, 0)] \\
 & + \mathcal{O}(B^{M+1}) .
 \end{aligned} \tag{10}$$

Note that for $N = 5$ the expansion becomes a bit more involved, but is still rather straightforward.

By looking at the ratio of the standard recursion relation and the B -expansion relation in Fig. 2 we can see clearly the numerical instability of the standard recursion relation when $-sB < 10^{-13}$. As can be seen from Fig. 1 we already can neglect terms of order B^3 in the B -expansion relation to achieve an accuracy of 10^{-25} in the integral evaluation. Also shown, in Fig. 3 is the imaginary part of the scalar integral using both recursion relations. As can be seen, the B -expansion relation can be used over a large range of values provided the expansion depth is sufficient (as indicated by Fig. 1).

We now can evaluate the $\gamma\gamma \rightarrow \gamma\gamma$ cross section in the forward region using both the standard and B -expansion relations. We define the normalized

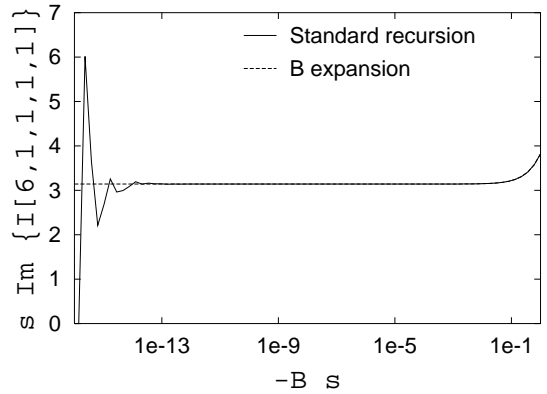


Figure 3. The value of $-sB$ vs the imaginary part of the 6-dimensional box integral, $I(6, 1, 1, 1, 1)$.

amplitude $A(\theta)$

$$\mathcal{M}(\theta) = \frac{e^4}{2\pi^2} A(\theta) \tag{11}$$

where e is the coupling strength of the photon-fermion vertex.

In Fig. 4 we show the helicity amplitude for $\gamma^+\gamma^+ \rightarrow \gamma^-\gamma^-$ scattering. In this case we have

$$A^{++;--}(\theta) = 1 . \tag{12}$$

As can be seen in Fig. 4, the standard recursion relation has a sudden loss in accuracy at around $\theta \approx 3 \times 10^{-3}$. On the other hand, the B expansion formula gives the correct result to within arbitrary precision.

Similarly, in Fig. 5 we show the helicity scattering $\gamma^+\gamma^+ \rightarrow \gamma^+\gamma^+$. The normalized helicity amplitude is now more complicated

$$\begin{aligned}
 A^{+++}(\theta) & = \frac{1+c^2}{4} \left[\log^2 \left(\frac{1-c}{1+c} \right) + \pi^2 \right] \\
 & + c \log \left(\frac{1-c}{1+c} \right) + 1
 \end{aligned} \tag{13}$$

where $c = \cos \theta$. The quantitative behaviour is identical to the previous case; the B improved recursion relations give an accurate result in the domain where numerical instabilities render the standard approach invalid.

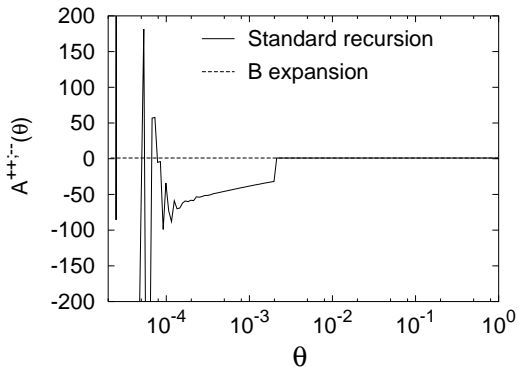


Figure 4. The scattering angle vs the normalized amplitude for $\gamma^+\gamma^+ \rightarrow \gamma^-\gamma^-$.

In summary, the B -expansion method can be used to extrapolate the algorithmic integration by parts method to all values of θ without any loss of accuracy.

4. Conclusions

The method outlined can readily be generalized to more complicated processes. As explained in sec. 2 this is done by rewriting the recursion relations as expansion in the small B -parameter or small eigenvalues of kinematic matrix. Because the recursion relations are numerically solved for each phase space point, the method allows exceptional kinematic configuration to be automatically detected by the algorithm on an event-by-event basis. If needed the algorithm can decide to use the expansion method without any knowledge of the underlying physics (e.g. threshold region, planar event configuration or other more complicated configurations). This is highly desirable because of the complexity of processes we are ultimately interested in. For example, four quark final states at hadron colliders such as $PP \rightarrow t\bar{t} + b\bar{b}$ have multiple mass thresholds and numerous other kinematic exceptional configurations. Similarly processes like $P\bar{P} \rightarrow W + 4$ jets requiring the evaluation of the complicated one-loop diagrams involving six partons plus a

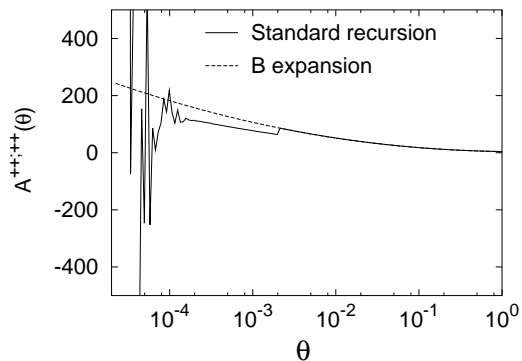


Figure 5. The scattering angle vs the normalized amplitude for $\gamma^+\gamma^+ \rightarrow \gamma^+\gamma^+$.

vector boson for which the exceptional kinematic configurations are difficult to comprehend.

The algorithm outlined in these proceedings augments the integration by parts algorithm of Ref. [2]. The combined numerical procedure should be able to calculate arbitrarily complicated one-loop amplitudes in *all* regions of phase space with arbitrary precision.

REFERENCES

1. K. G. Chetyrkin and F. V. Tkachov, Nucl. Phys. B 192 (1980) 159; Z. Bern, L. J. Dixon and D. A. Kosower, Nucl. Phys. B 412 (1994) 751; J. Fleischer, F. Jegerlehner and O. V. Tarasov, Nucl. Phys. B 566 (2000) 423; T. Binoth, J. P. Guillet and G. Heinrich, Nucl. Phys. B 572 (2000) 362; G. Duplancic and B. Nizic, Eur. Phys. J. C35 (2004) 105; F. del Aguila and R. Pittau, arXiv:hep-ph/0404120.
2. W.T. Giele and E.W.N. Glover, JHEP 0404, 029 (2004).
3. J.M. Campbell, E.W.N. Glover and D.J. Miller, Nucl. Phys. B 498 (1997) 397.
4. A. Ferroglia, M. Passera, G. Passarino and S. Uccirati, Nucl. Phys. B 650 (2003) 162.